Communication

Lowering Strain Rate Simultaneously Enhances Carbon- and Hydrogen-Induced Mechanical Degradation in an Fe-33Mn-1.1C Steel

IBRAHIM BURKAY TUĞLUCA, MOTOMICHI KOYAMA, YUSAKU SHIMOMURA, BURAK BAL, DEMIRCAN CANADINC, EIJI AKIYAMA, and KANEAKI TSUZAKI

We investigated the strain rate dependency of the hydrogen-induced mechanical degradation of Fe-33Mn-1.1C steel at 303 K within the strain rate range of 10^{-2} to 10^{-5} s^{-1}. In the presence of hydrogen, lowering the strain rate monotonically decreased the work hardening rate, elongation, and tensile strength and increased the yield strength. Lowering the strain rate simultaneously enhanced the plasticity-related effects of hydrogen and carbon, leading to the observed degradation of the ductility.

https://doi.org/10.1007/s11661-018-5080-7

The quest for new steels lighter and stronger than conventional alloys has been ongoing as a part of the drive for improved energy efficiency. In 1888, Sir Robert Hadfield demonstrated the importance of the simultaneous addition of high concentrations of manganese and carbon in austenitic steels, resulting in an improved work hardening rate and associated uniform elongation.[1] In this context, it is known that the major roles of manganese and carbon in work hardening are triggering deformation twinning[2,3] and dynamic strain aging (DSA).[4–6] Furthermore, austenitic steels containing high concentrations of manganese and carbon have been noted as hydrogen-resistant, high-strength steels used for hydrogen-energy-related infrastructures; this is due to the close-packed fcc structure, which exhibits a low diffusivity of hydrogen.[7] Thus, in light of these two energy-related aspects, the intrinsic effects of manganese, carbon, and hydrogen on strength and ductility have been of great concern for steel scientists and engineers.

Regarding the effects of carbon, we have found that a high concentration of interstitial carbon degrades the ductility of austenitic high-manganese steels, even without hydrogen uptake, when the stacking fault energy is relatively high and the strain rate is below 10^{-3} s^{-1}.[8] For instance, an Fe-33Mn-1.1C* steel satisfies this condition. The main cause of this behavior was determined to be deformation heterogeneity, associated with DSA-induced Portevin–Le Chatelier (PLC) effect. Moreover, even at a high strain rate of around 10^{-2} s^{-1}, where the PLC banding effect is not significant, hydrogen uptake causes remarkable mechanical degradation, which is associated with deformation localization.[9] In this context, our special interest in this study is to determine whether lowering the strain rate can simultaneously enhance the carbon and hydrogen-induced mechanical degradation in a high-manganese steel, which contains a high amount of interstitial carbon. According to a previous study of an Fe-23Mn-0.5C twinning-induced plasticity steel, the effect of hydrogen on mechanical degradation must be more pronounced when the strain rate is lowered to below 10^{-3} s^{-1}.[10] In Ni-C face-centered cubic (fcc) alloys, interstitial carbon can suppress the effects of hydrogen on the increase in dislocation mobility[11] and mechanical degradation[12] at low strain rates. Based on these considerations, we present strain rate dependency of the hydrogen embrittlement susceptibility of the Fe-33Mn-1.1C steel.

An ingot of the Fe-33Mn-1.1C steel was prepared by vacuum induction melting, which was then forged and rolled at 1273 K. The rolled bar was solution treated at 1273 K for 1 hour, followed by water quenching. The average grain size was measured to be 33 μm. The detailed chemical composition and microstructure have been presented elsewhere.[9] Tensile specimens were extracted from the bar by electric discharge machining

*All chemical contents are provided in weight percentage, unless otherwise noted.

IBRAHIM BURKAY TUĞLUCA is with the Department of Mechanical Engineering, Kyushu University, Nishi-ku Fukuoka 918-0395, Japan and also with the Department of Mechanical Engineering, Abdullah Gül University, 38080 Kayseri, Turkey. MOTOMICHI KOYAMA and YUSAKU SHIMOMURA are with the Department of Mechanical Engineering, Kyushu University. Contact e-mail: koyama@mech.kyushu-u.ac.jp BURAK BAL is with the Department of Mechanical Engineering, Abdullah Gül University. DEMIRCAN CANADINC is with the Department of Mechanical Engineering, Koç University, Sariyer, Istanbul 34450, Turkey. EIJI AKIYAMA is with the Institute for Materials Research, Tohoku University, Katahira 2-1-1, Aoba-ku, Sendai 980-8577, Japan. KANEAKI TSUZAKI is with the Department of Mechanical Engineering, Kyushu University and also with the HYDROGENIOUS, Kyushu University, Motooka 744, Nishi-ku, Fukuoka 819-0395, Japan.

Manuscript submitted May 25, 2018.
Article published online January 2, 2019

(EDM) to the gauge geometry featuring 4 mm width, 1 mm thickness, and 30 mm length. The EDM-affected layer was removed by chemical polishing with a H_2O_2:HF = 10:1 solution.

Tensile tests were carried out at a temperature of 303 K and at initial strain rates of 10^{-2}, 10^{-3}, 10^{-4}, and 10^{-5} s^{-1} with and without hydrogen pre-charging. The deformation temperature was controlled by a thermostatic chamber attached to the tensile testing machine. Furthermore, the strain distributions in the specimens without hydrogen pre-charging were measured at 20 pct macroscopic strain by digital image correlation (DIC). The random pattern used to apply the DIC method was formed by using a black spray on a specimen undercoated with white enamel. Prior to the tensile deformation experiments, hydrogen was introduced by electrochemical charging at 353 K for 72 hours in a 3 pct NaCl aqueous solution containing 3 g/L NH_4SCN. The current density was fixed at 100 A m^{-2} with a platinum wire acting as the counter electrode. In order to remove a thin contamination layer formed on the specimen surface during hydrogen charging, the specimens were mechanically polished only with water on buff for 20 minutes every 12 hours. After this water-polishing process, the thickness of the specimens did not change, but a shiny surface appeared. For the mechanical polishing with water, hydrogen charging was stopped for 25 minutes every 12 hours. The tensile tests were carried out within 30 minutes after the hydrogen pre-charging. The diffusible hydrogen content was 44.0 ppm, which was measured by thermal desorption spectroscopy from room temperature up to 573 K.[9] After the tensile tests, the fracture surfaces of the post-mortem specimens were characterized using scanning electron microscopy.

The tensile deformation experiments (Figure 1(a)) showed that lowering the strain rate degrades the tensile ductility even without hydrogen charging, which is attributed to deformation heterogeneity associated with the carbon-induced PLC banding.[8] The hydrogen charging decreased the elongation and flow stress and increased the yield strength, irrespective of the strain rate. The increase of the 0.2 pct proof stress due to hydrogen charging was estimated to be 5, 1, 4, and 7 pct

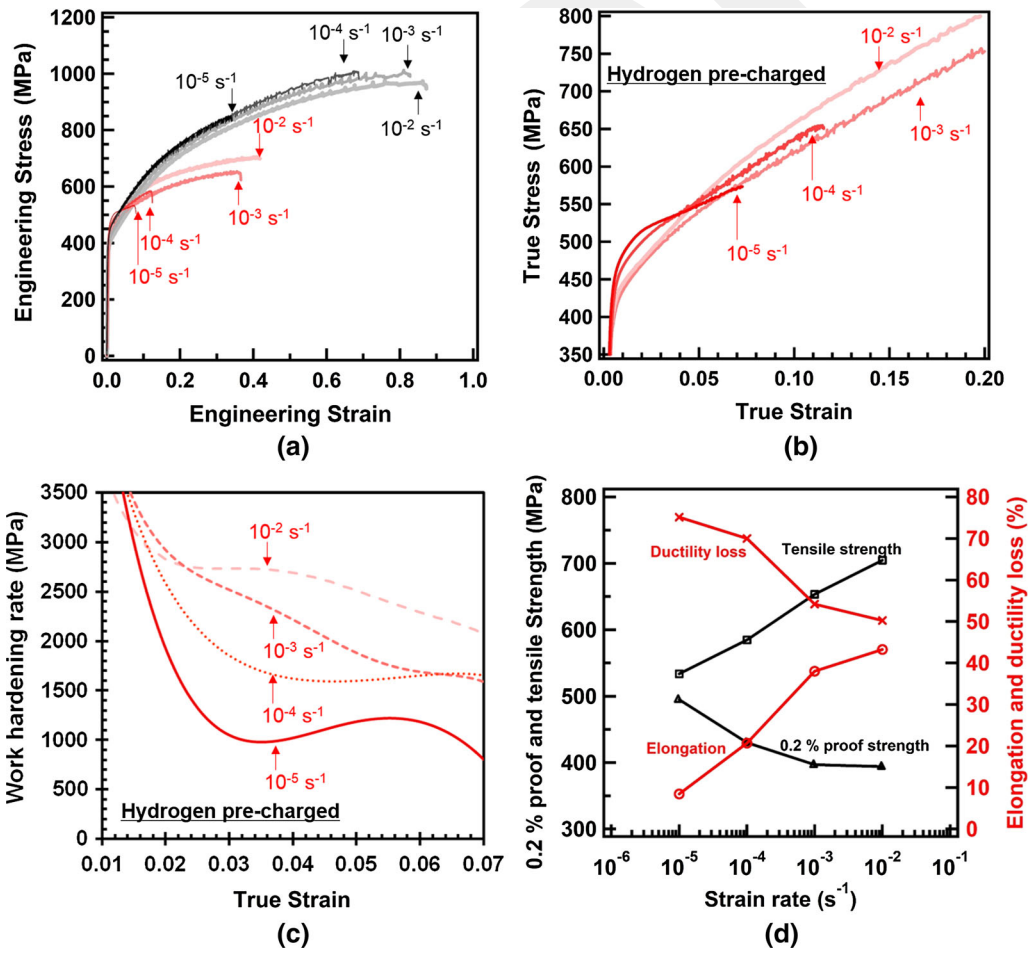

Fig. 1—(*a*) Engineering stress–engineering strain curves with and without hydrogen charging. The black/gray and red curves indicate the results without and with hydrogen charging, respectively. (*b*) True stress–true strain curves with hydrogen charging up to 0.2 true strain and (*c*) work hardening curves with hydrogen charging up to a true strain of 0.07. (*d*) Strain rate dependence of the tensile properties of the hydrogen-charged specimen and the magnitude of the hydrogen-induced ductility loss (Color figure online).

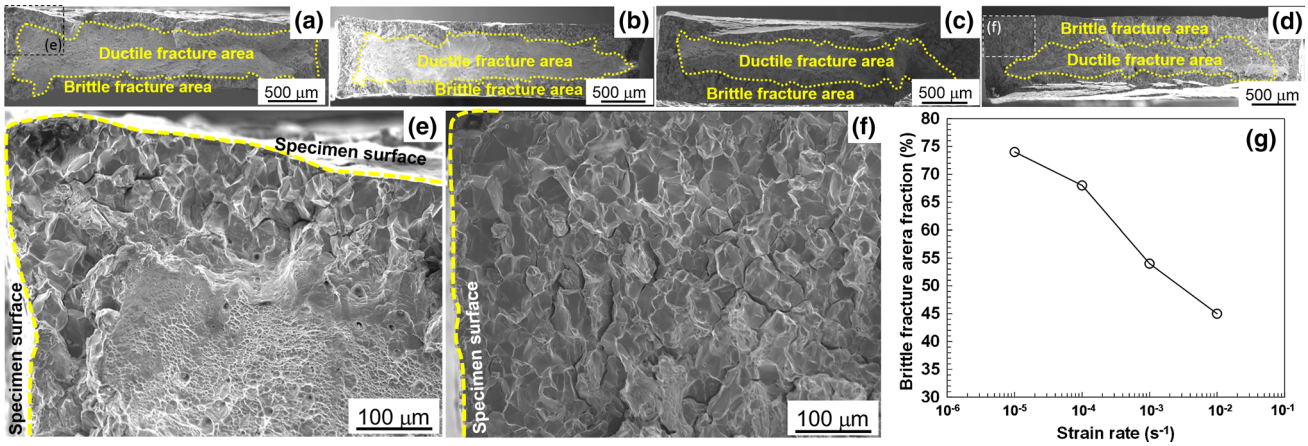

Fig. 2—Overviews of the fracture surfaces obtained at (*a*) 10^{-2}, (*b*) 10^{-3}, (*c*) 10^{-4}, and (*d*) 10^{-5} s^{-1}. The dashed lines indicate the boundaries between the ductile and brittle fracture areas. Magnified images of the left upper corner of the surface at strain rates of (*e*) 10^{-2} and (*f*) 10^{-5} s^{-1}. (*g*) Fraction of brittle fracture area plotted against strain rate.

for strain rates of 10^{-2}, 10^{-3}, 10^{-4}, and 10^{-5} s^{-1}, respectively. The effects of strain rate on these respective hydrogen effects can be seen clearly in Figures 1(b) and (c): both elongation to failure and work hardening rate decreased with decreasing strain rate, while the yield strength increased.

Figure 1(d) quantitatively summarizes the mechanical properties of the hydrogen-charged specimens at different strain rates. Here, we note the strain rate dependence of ductility loss, and the ductility loss is defined as

$$\Delta\varepsilon = \frac{\varepsilon_0 - \varepsilon_{\text{withH}}}{\varepsilon_0}, \qquad [1]$$

where ε_0 and $\varepsilon_{\text{withH}}$ are the total elongations without and with hydrogen charging, respectively. The negative strain rate dependence of the ductility loss indicates that the effects of both carbon and hydrogen on mechanical degradation were enhanced at lower strain rates.

The work hardening capacity of Fe-Mn-C-based austenitic steels has been reported to increase with decreasing strain rate because of the promotion of DSA,[5,6,13] which is consistent with the present results obtained without hydrogen pre-charging. In contrast, the work hardening rate of the hydrogen-charged specimens decreased with decreasing strain rate. A previous study revealed that the presence of hydrogen in the steel at an initial strain rate of 10^{-2} s^{-1} decreased the apparent work hardening rate because of the decreased cross-sectional area resulting from the formation of numerous surface cracks.[9] More specifically, the reduction in the work hardening rate could be explained based on one assumption: the ductile fracture area on the fracture surface is regarded as the remaining cross-sectional area at the fracture strain. Figures 2(a) through (d) show the fractographs of the hydrogen-charged specimens for different strain rates. Both brittle and ductile fracture features are observed, and we note here that the brittle fracture area increases with decreasing strain rate. The magnified images shown in Figures 2(e) and (f) more clearly indicate this increase in the brittle fracture area as the strain rate decreases from 10^{-2} to 10^{-5} s^{-1}. Figure 2(g) shows a summary of the quantitative estimates of the strain rate sensitivity of the brittle fracture area. Accordingly, if compared at the same strain of 0.08, which corresponds to the fracture elongation at the strain rate of 10^{-5} s^{-1} with hydrogen, the brittle crack propagated more significantly when the strain rate was lower. Therefore, the flow stress and the work hardening rate decreased with decreasing strain rate due to the reduction in remaining cross-sectional area.

Another characteristic change in the macroscopic deformation behavior observed after hydrogen uptake is an increase in the yield strength. This increase in yield strength has been reported to stem from the solution hardening of hydrogen in austenitic steels[14] and fcc Ni alloys.[15,16] However, solution hardening by hydrogen alone cannot explain the increase in yield strength observed with decreasing strain rate, which is inversely related to other considerations, based on the thermally activated process of dislocation motion.

With this motivation, we discuss a strain-rate-dependent hardening mechanism. First, note that there are generally a significant number of pre-existing dislocations in steels, and in carbon steels annealed without rapid cooling, an interaction between the pre-existing dislocations and carbon during furnace/air cooling controls the upper yield strength.[17] Therefore, the negative strain rate sensitivity of the yield strength can be attributed to the interaction between pre-existing dislocations and solute hydrogen in the present case. In terms of hydrogen-dislocation competitive motion, the drag force on the dislocation by the solute hydrogen is key to understanding the strain rate dependence.[11] Occurrence of a drag force requires two conditions: (1) formation of hydrogen atmospheres at the dislocations and (2) the hydrogen atmospheres move with but lag behind the dislocations. Therefore, the drag force increases with decreasing strain rate owing to the formation of a hydrogen atmosphere at the dislocation. Then, the drag force decreases with decreasing strain

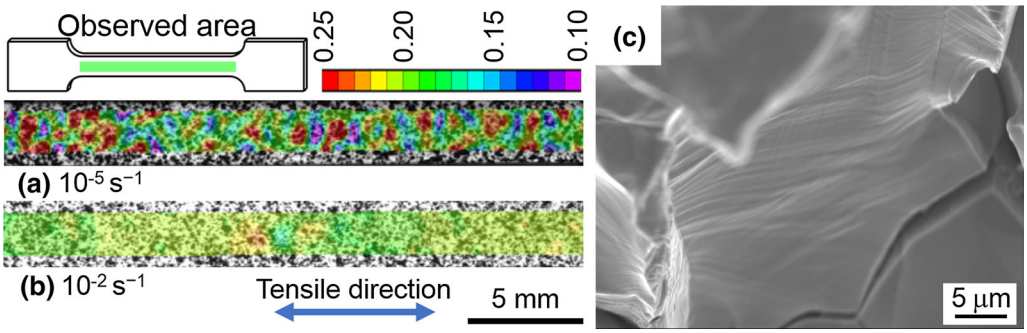

Fig. 3—(*a*) Distribution of strain along the tensile direction in the hydrogen-uncharged specimens deformed up to 20 pct macroscopic strain at strain rates of (a) 10^{-5} and (*b*) 10^{-2} s^{-1}. The green part of the specimen schematically indicates the region used for the DIC analyses. (*c*) Fractography image showing slip traces on the intergranular fracture region in the hydrogen-charged specimen deformed at the strain rate of 10^{-5} s^{-1} (Color figure online).

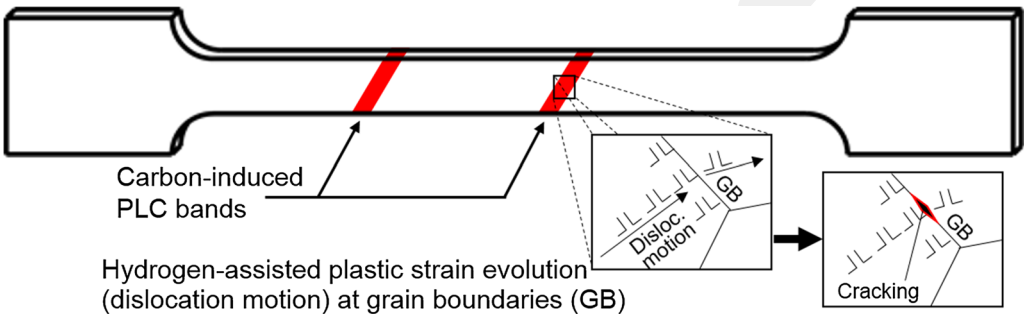

Fig. 4—Schematics of deformation heterogeneity at the low strain rate.

rate due to a reduction in the lag between the motion of the dislocation and hydrogen. The former strain rate dependence of the drag stress explains the negative strain rate sensitivity of the yield strength.

In terms of elongation and ductility loss, deformation heterogeneity is key to revealing the underlying mechanisms of the carbon and hydrogen effects. Figures 3(a) and (b) show the strain distributions at 20 pct macroscopic strain during deformation at strain rates of 10^{-5} and 10^{-2} s^{-1} without hydrogen pre-charging. The specimen tested at the strain rate of 10^{-5} s^{-1} exhibited sub-millimeter-scale deformation heterogeneity, while significant deformation heterogeneity was not observed at the strain rate of 10^{-2} s^{-1}. This indicates that lowering the strain rate enhances carbon-induced deformation heterogeneity, *i.e.*, PLC banding. This sub-millimeter scale deformation heterogeneity results in premature ductile fractures with dimple surfaces and does not cause brittle cracking in the Fe-33Mn-1.1C steel.[8] In fact, micro-damage, such as a crack or void, evolves with the plastic strain in Fe-Mn-C austenitic steels even before the external stress reaches the tensile strength.[18,19] Since the damage evolution is a plastic-strain-dependent phenomenon, micro-damage appears preferentially in the PLC band where the strain is locally high.[20] The micro-damage growth determines the work hardening behavior and associated elongation in Fe-Mn-C austenitic steels.[19,20] In this regard, premature ductile fracture occurs at a low strain rate when the maximum local strain in the PLC band reaches a failure strain under uniform deformation, such as the 10^{-2} s^{-1} case. As mentioned above, hydrogen charging does cause brittle cracking, and the fraction of brittle fracture area was found to increase with decreasing strain rate. The brittle crack surface involves a considerable number of slip traces as shown in Figure 3(c), which has been observed when plasticity-driven intergranular cracking occurs in pure Ni[21] and high-Mn steel.[22] This indicates that lowering the strain rate assists the plasticity-driven brittle-like cracking along microstructural interfaces such as grain boundaries. Since the brittle-like cracking did not occur when hydrogen was not introduced, hydrogen contributes to the occurrence of the plasticity-driven cracking. More specifically, the hydrogen-assisted cracking would occur within the carbon-induced PLC bands (as shown schematically in Figure 4), which explains how the effects of carbon and hydrogen simultaneously facilitate the observed strain rate effect on mechanical degradation.

In conclusion, lowering the strain rate from 10^{-2} to 10^{-5} s^{-1} assists both the carbon- and hydrogen-induced localized plasticity in Fe-33Mn-1.1C austenitic steel, which causes remarkable mechanical degradation. More specifically, lowering the strain rate with hydrogen significantly decreases the work hardening rate, elongation to failure, and tensile strength, while the yield strength is increased. The decrease in work hardening rate with decreasing strain rate results from acceleration of hydrogen-assisted brittle crack growth that causes a reduction in the cross-sectional area of the specimens at each strain level. On the other hand, the increase in yield

strength with decreasing strain rate cannot be concluded here. In terms of local phenomena, decreasing the strain rate enhances carbon-induced deformation heterogeneity, *i.e.*, PLC banding, and simultaneously enhances hydrogen-assisted plasticity-driven intergranular cracking. The combined effects of carbon and hydrogen result in the remarkable degradation of elongation when the strain rate is decreased in the presence of hydrogen.

This work was financially supported by the Japan Science and Technology Agency (JST) (Grant No.: 20100113) under Industry-Academia Collaborative R&D Program ''Heterogeneous Structure Control: Towards Innovative Development of Metallic Structural Materials'' and JSPS KAKENHI (JP16H06365 and JP17H04956). B. Bal acknowledges the financial support by the AGU-BAP under Grant Number: FAB-2017-77.

REFERENCES

1. RA Hadfield: *Manganese-steel: I. Manganese in its application to metallurgy: II. Some newly-discovered properties of iron and manganese*, Westminster, Institution, 1888.
2. O. Bouaziz, S. Allain, and C. Scott: *Scripta Mater.*, 2008, vol. 58, pp. 484–87.
3. D.R. Steinmetz, T. Jäpel, B. Wietbrock, P. Eisenlohr, I. Gutierrez-Urrutia, A. Saeed-Akbari, T. Hickel, F. Roters, and D. Raabe: *Acta Mater.*, 2013, vol. 61, pp. 494–510.
4. P. Chowdhury, D. Canadinc, and H. Sehitoglu: *Mater. Sci. Eng. R*, 2017, vol. 122, pp. 1–28.
5. Y. Dastur and W. Leslie: *Metall. Trans.*, 1981, vol. 12A, pp. 749–59.
6. S.-J. Lee, J. Kim, S.N. Kane, and B.C. De Cooman: *Acta Mater.*, 2011, vol. 59, pp. 6809–19.
7. M. Koyama, E. Akiyama, Y.-K. Lee, D. Raabe, and K. Tsuzaki: *Int. J. Hydrog. Energy*, 2017, vol. 42, pp. 12706–23.
8. M. Koyama, Y. Shimomura, A. Chiba, E. Akiyama, and K. Tsuzaki: *Scripta Mater.*, 2017, vol. 141, pp. 20–23.
9. I.B. Tuğluca, M. Koyama, B. Bal, D. Canadinc, E. Akiyama, and K. Tsuzaki: *Mater. Sci. Eng. A*, 2018, vol. 717, pp. 78–84.
10. B. Bal, M. Koyama, G. Gerstein, H.J. Maier, and K. Tsuzaki: *Int. J. Hydrog. Energy*, 2016, vol. 41, pp. 15362–72.
11. E. Sirois and H.K. Birnbaum: *Acta Metall. Mater.*, 1992, vol. 40, pp. 1377–85.
12. A. Kimura and H.K. Birnbaum: *Acta Metall.*, 1988, vol. 36, pp. 757–66.
13. D. Canadinc, C. Efstathiou, and H. Sehitoglu: *Scripta Mater.*, 2008, vol. 59, pp. 1103–06.
14. D.P. Abraham and C.J. Altstetter: *Metall. Mater. Trans.*, 1995, vol. 26A, pp. 2849–58.
15. H.K. Birnbaum and P. Sofronis: *Mater. Sci. Eng. A*, 1994, vol. 176, pp. 191–202.
16. J. Eastman, F. Heubaum, T. Matsumoto, and H.K. Birnbaum: *Acta Metall.*, 1982, vol. 30, pp. 1579–86.
17. A.H. Cottrell: *Dislocations and Plastic Flow in Crystals*, Oxford University Press, New York, 1954.
18. F. Fabrègue, C. Landron, O. Bouaziz, and E. Maire: *Mater. Sci. Eng. A*, 2013, vol. 579, pp. 92–98.
19. C.L. Yang, Z.J. Zhang, P. Zhang, and Z.F. Zhang: *Acta Mater.*, 2017, vol. 136, pp. 1–10.
20. H.-Y. Yu, S.-M. Lee, J.-H. Nam, S.-J. Lee, D. Fabrègue, M.-H. Park, N. Tsuji, and Y.-K. Lee: *Acta Mater.*, 2017, vol. 131, pp. 435–44.
21. M.L. Martin, B.P. Somerday, R.O. Ritchie, P. Sofronis, and I.M. Robertson: *Acta Mater.*, 2012, vol. 60, pp. 2739–45.
22. M. Koyama, H. Springer, S.V. Merzlikin, K. Tsuzaki, E. Akiyama, and D. Raabe: *Int. J. Hydrog. Energy*, 2014, vol. 39, pp. 4634–46.